Sjögren's syndrome-associated SNPs increase GTF2I expression in salivary gland cells to enhance inflammation development

Shuhei Shimoyama[1,2*], Ikuma Nakagawa[1,2*], Jing-Jing Jiang[1,3], Isao Matsumoto[4], John A. Chiorini[5], Yoshinori Hasegawa[6], Osamu Ohara[6], Rie Hasebe[7], Mitsutoshi Ota[1], Mona Uchida[1], Daisuke Kamimura[1], Shintaro Hojyo[1], Yuki Tanaka[1], Tatsuya Atsumi[2], and Masaaki Murakami[1]

[1]Division of Molecular Psychoimmunology, Institute for Genetic Medicine, Hokkaido University, Sapporo, Japan
[2]Department of Rheumatology, Endocrinology and Nephrology, Hokkaido University Graduate School of Medicine, Sapporo, Japan
[3]Institute of Preventive Genomic Medicine, School of Life Sciences, Northwest University, Xian 710069, China
[4]Division of Clinical Immunology, Major of Advanced Biological Applications, Graduate School Comprehensive Human Science, University of Tsukuba, Tsukuba, Japan
[5]AAV Biology Section, Division of Intramural Research, National Institute of Dental and Craniofacial Research, National Institutes of Health, Bethesda, MD, USA
[6] Laboratory of Clinical Omics Research, Department of Applied Genomics, Kazusa DNA Research Institute, 2-6-7 Kazusa-kamatari, Kisarazu, Chiba, Japan
[7]Biomedical Animal Research Laboratory, Institute for Genetic Medicine, Hokkaido University, Sapporo, Japan

* Equal contribution

Address corresponded to:
Masaaki Murakami
N15 W7, kita-ku, Sapporo, Hokkaido 060-8638, Japan
Phone : +81-11-706-5120
Fax : +81-11-706-7542
e-mail : murakami@igm.hokudai.ac.jp

Running title
NF-κB activation in salivary glands by GTF2I

Keywords
GTF2I, IL-6 amplifier, Sjögren's syndrome, NF-κB

Abstract

Sjögren's syndrome (SS) is an autoimmune disease characterized by inflammation, lymphoid infiltration, and destruction of the salivary glands. Although many genome-wide association studies have revealed disease-associated risk alleles, the functions of the majority of these alleles are unclear. Here, we show previously unrecognized roles of GTF2I molecules by using two SS-associated SNPs, rs73366469 and rs117026326 (GTF2I SNPs). We found that the risk alleles of GTF2I SNPs increased GTF2I expression and enhanced NF-κB activation in human salivary gland cells via the NF-κB p65 subunit. Indeed, the knockdown of GTF2I suppressed inflammatory responses in mouse endothelial cells and in vivo. Conversely, the overexpression of GTF2I enhanced NF-κB reporter activity depending on its p65-binding N-terminal leucine-zipper domain. GTF2I is highly expressed in the human salivary gland cells of SS patients expressing the risk alleles. Consistently, the risk alleles of GTF2I SNPs were strongly associated with activation of the IL-6 amplifier, which is hyperactivation machinery of the NF-κB pathway, and lymphoid infiltration in the salivary glands of SS patients. These results demonstrated that GTF2I expression in salivary glands is increased in the presence of the risk alleles of GTF2I SNPs, resulting in activation of the NF-κB pathway in salivary gland cells. They also suggest that GTF2I could be a new therapeutic target for SS.

Introduction

Sjögren's syndrome (SS) is an inflammatory autoimmune disease that is characterized by sicca symptoms such as dry eyes and dry mouth. Lymphocyte infiltration in the salivary glands or lacrimal glands of SS patients is often reported (1,2). However, how T cells and B cells accumulate and induce inflammation in the secretory glands during SS development has not been shown. Moreover, the roles of secretary gland cells in the development of SS are just beginning to be investigated.

Inflammatory cytokines are likely involved in the development of SS. Studies have reported an increased concentration of inflammatory cytokines including TNFα, IL-6, and IL-17A in the tear fluid of SS patients (3) and an elevation of IL-17A levels in both the serum and salivary glands (4). However, a detailed molecular mechanism explaining how cytokines and chemokines are upregulated in the salivary glands and how they induce inflammation development during SS development has not been shown.

We previously found that IL-6, TNFα, and IL-17A stimulations enhance the expression of inflammatory cytokines and chemokines in nonimmune cells followed by the development of inflammatory diseases (5,6). This synergistic effect is mediated by the simultaneous activation of NF-κB and STAT3 in the cells. IL-6 is an exclusive STAT3 stimulator, but several NF-κB stimulators have been observed during inflammation development, including in two CD4+ T cell-mediated disease models, EAE and EAU (5,7). Accordingly, the IL-6 amplifier describes the molecular mechanism that activates this synergistic effect (5). Since its original discovery, evidence of the IL-6 amplifier has been found in many mouse disease models and patient samples of arthritis, multiple sclerosis, psoriasis, uveoretinitis, and chronic rejection, and also human samples from patients suffering from many of the same and other inflammatory diseases (6,8-23).

A later genome-wide screening to identify the genes that regulate the IL-6 amplifier found about 1,200 positive regulators and 500 target genes (5,18). The candidate regulatory genes included eight genes that were identified in GWAS studies of primary SS patients (BLK, CXCR5, IL-12A, IRF5, STAT4, TNIP, TNFAIP3, and GTF2I) (24-27). In particular, little is known about the role of GTF2I in autoimmune diseases including SS.

In the present work, we show that SS patients with the risk alleles show more GTF2I expression and more NF-κB and STAT3 activation in salivary gland cells and more accumulation of lymphocytes, most likely via chemokine expression, in salivary glands. Mechanistic analysis showed that GTF2I in nonimmune cells enhanced the recruitment of transcriptional regulators to the promoters of NF-κB target genes including various chemokines as well as IL-6. By directly binding to NF-κB p65, GTF2I activated the NF-κB pathway to induce inflammation. These results suggest GTF2I in salivary gland cells could be a potential therapeutic target for SS.

Material and Methods

Mouse strains

C57BL/6 mice were purchased from Japan SLC. F759 mice that possess a human gp130 variant (S710L) were previously established (6). F759 mice were backcrossed with C57BL/6 mice for more than 10 generations. All mice were maintained under specific pathogen-free conditions according to the protocol of Hokkaido University. All of the protocols for mouse experiments were approved by the Institutional Animal Care and Use Committee of Hokkaido University under the approval of research No. 20-0003, and the experiments were performed following the guidelines of the Committee. The mice used in the experiments were 6-8-weeks old.

Human salivary gland sample preparation and GTF2I SNP genotyping

Human samples from labial gland biopsies were used under protocols approved by the Human Ethics Committee of Hokkaido University Hospital and Tsukuba University Hospital under the approval of research No. 014-0466. Labial gland tissue specimens were acquired by lip biopsy, fixed by PAXgene Tissue Containers (QIAGEN) for 2 h, and stored in PAXgene Tissue Stabilizer (QIAGEN) at -20˚C until use. The diagnosis of SS was based on the American College of Rheumatology/European League Against Rheumatism classification criteria for primary SS (28). Genotyping of the GTF2I SNPs was performed as follows. Human salivary gland samples were excised (about 6 mg) and used for checking the existence of two SNPs (rs117026326 and rs73366469), which were highly observed in SS, rheumatoid arthritis and systemic lupus erythematosus patients (Supplementary Figure 1A) (24-26). Genome DNA was extracted with a DNA/RNA Mini Kit (QIAGEN) according to the manufacturer's protocol. PCR and SNP-specific sequencing were performed using KOD Fx (TOYOBO) and the BigDye Terminator v3.1 Cycle Sequencing Kit (Applied Biosystems). The sequences of the primers specific for the two types of SNPs are shown in Table 1.

Cell lines and stimulation conditions

A type 1 collagen^{+} mouse endothelial cell line (BC-1) was obtained from Dr. M. Miyasaka (Osaka University). Primary human synoviocytes were purchased from ScienCell Research Laboratories and immortalized with the transfection of SV40 large T antigen. A human salivary gland cell line was obtained from Dr. I. Matsumoto (Tsukuba University). All of the cell lines were cultured in Dulbecco's modified eagle medium (DMEM; Thermo Fisher Scientific) with 10% fetal bovine serum (FBS; Thermo Fisher Scientific) without antibiotics at 37˚C under 5% CO_2.

For cytokine stimulation, the cells were plated in 96-well plates, 6-well plates or a 100-mm dish, stimulated with human IL-6 (100 ng/ml; Toray Industries) plus human or mouse soluble IL-6 receptor (IL-6R; 100 ng/ml; R&D Systems) and/or human or mouse IL-17A (50 ng/ml; R&D Systems); human or mouse TNFα (100 ng/ml; PeproTech); LPS (100 ng/ml; Sigma Aldrich); CpG (5 μM; Novus biologicals); poly (I:C) (200 ng/ml; R&D Systems); or R848 (500 ng/ml; Sigma Aldrich) after 2-24 h of serum starvation. Stimulation times are described in the figure legends.

Antibodies

The following antibodies (Abs) were used for the western blotting, immunoprecipitation (IP), chromatin immunoprecipitation (ChIP), confocal microscopy, and

immunohistochemistry: anti-GTF2I (ab88864 for western blotting, Abcam), anti-GTF2I-C-terminal (ab135619 for immunohistochemistry, Abcam), anti-p65 (C-20, Santa Cruz), anti-phospho-p65 (Ser536 93H1, Cell Signaling Technology), anti-IκBα (Cell Signaling Technology), anti-phospho-IκBα (Ser32/36 5A5, Cell Signaling Technology), anti-STAT3 (Cell Signaling Technology), anti-phospho-STAT3 (Cell Signaling Technology), anti-FLAG M2 (Sigma Aldrich), anti-c-Myc (Sigma Aldrich), anti-acetyl H3K9 antibody (Sigma Aldrich), anti-trimethyl H3K27 antibody (Sigma Aldrich), Alexa Fluor 488 goat anti-rabbit IgG (H+L) (Invitrogen), Alexa-Fluor 546 goat-anti-mouse IgG (H+L) (Invitrogen), and Hoechst 33342 trihydrochloride trihydrate (Life Technologies).

Immunohistochemistry

Human salivary gland tissues were embedded in paraffin and sectioned at a thickness of 5 μm. The sections were deparaffinized using xylene and dehydrated using ethanol. Heat-induced antigen retrieval was performed with sodium citrate. Endogenous peroxidase activity was blocked with 3% H_2O_2. The treated sections were rinsed and incubated 1 h for blocking with goat serum (Vector laboratories) in TBS-0.1% Tween. Subsequently, the sections were incubated with anti-phospho-NF-κB p65, anti-phospho-STAT3, anti-GTF2I, or control antibodies overnight at 4˚C. After washing, the secondary biotinylated anti-rabbit IgG or anti-mouse IgG antibodies (Vector laboratories) were added. The ImmPACT DAB Kit (Vector laboratories) was used to detect the antigens. Sections were also stained with hematoxylin and eosin. Quantification was performed by ImageJ software.

Cytokine-induced arthritis in F759 mice

The joints were injected with lentivirus carrying two kinds of shRNA specific for mouse Gtf2i (n = 4, each) or a scrambled sequence (Sigma-Aldrich, n = 8) on days 0, 2, and 4. IL-17A (R&D Systems) and IL-6 (Toray Industries) or saline were injected into the ankle joints of F759 mice as previously described (10-14,16,18,21) on days 5, 7, and 9. The clinical assessment of arthritis in mice injected with the cytokines and/or shRNA-carrying lentivirus were done as previously described (10-13,16,18,21). In brief, the severity of the arthritis was determined based on two bilaterally assessed parameters: (1) swelling in the ankle and (2) restricted mobility of the ankle joints. The severity of each parameter was graded on a scale of 0–3, where 0 indicates no change; 1, mild change; 2, medium change; and 3, severe change. Averages for a single point in one leg ankle joint from each mouse were used for the clinical assessments. Synovial tissue fragments were separated using Liberase TM (100 μg/ml; Sigma-Aldrich) in RPMI in a 37 ℃ water bath for 30 min (n=3, each group).

Real-time PCR

The 7300 fast real-time PCR system (Applied Biosystems) and SYBR Green PCR master mix (Kapa Biosystems) were used to quantify the expression levels of target mRNA and internal control mRNA (hypoxanthine phosphoribosyltransferase (HPRT) for mouse cell lines, and glycerol-3-phosphatase dehydrogenase (GAPDH) for human cell lines or human tissue samples). The cells were plated in 12-well plates (1×10^5 cells/well) and stimulated with 100 ng/ml of human IL-6 (Toure) plus 100 ng/ml of soluble IL-6R (R&D Systems), 50 ng/ml of mouse IL-17A (R&D Systems) or 50 ng/ml of TNFα (PeproTech) for 3 h after 2 h of serum starvation. Total RNA was prepared from the cells using a GenElute mammalian total RNA Kit and DNase I (Sigma-Aldrich). The PCR primer pairs used for the real-time PCR are described in Table 2. The conditions for real-time PCR were 40 cycles at 94˚C for 15 sec followed by 40 cycles at 60˚C for 60 sec. The relative mRNA expression levels were normalized to the levels of HPRT or GAPDH mRNA expression.

Enzyme-linked immunosorbent assay (ELISA)

The IL-6 concentration in the cell-culture supernatant after stimulation with IL-6 and IL-17A or TNFα was determined with an ELISA Kit (BD Biosciences) according to the manufacturer's protocol. The detection range was 15.625-1000 pg/ml. Concentrations

were calculated using a standard curve generated with specific standards provided by the manufacturer. Each sample was measured in duplicate.

MTT assay

Cell growth was determined with thiazolyl blue tetrazolium bromide according to the manufacturer's protocol (Sigma-Aldrich).

GTF2I shRNA knockdown cells

BC-1 cells were cultured on day 1 in a 96-well flat-bottom plate (1000 cells/well) in 100 µl of DMEM containing 10% FBS. The medium was replaced on day 2 with a DMEM containing lentivirus carrying 1 µl of gene-specific shRNA (nontarget shRNA, Sigma Mission SHC002V; GTF2I shRNA-1, TRCN0000086101, CCGGGACCCTGATTACTATCAGTATCTCGAGATACTGATAGTAATCAGGGTC TTTTTG; and GTF2I shRNA-2, TRCN0000086102, CCGGCCAGCAGAAGATTCTACTCAACTCGAGTTGAGTAGAATCTTCTGCTGG TTTTTG; Sigma Aldrich), 10% FBS, and 8 µg/ml Polybrene. On day 3, 200 µl of DMEM containing 10% FBS and 5 µg/ml puromycin was added to each well.

Human small interfering RNAs

Small interfering RNAs (siRNAs) were transfected into HeLa cells or immortalized human synoviocytes using Lipofectamine RNAiMAX (Thermo Fisher Scientific). To verify the knockdown efficiency, RT-PCR analysis of the respective target was performed. The sequences for the sense oligonucleotides of the most effective knockdown constructs are as follows: human si-GTF2I (SASI_Hs02_00332037; Sigma-Aldrich), human si-p65 (SASI_Hs01_00171090; Sigma–Aldrich), and human si-nontarget (Sigma Mission SIC-001s; Sigma-Aldrich).

Western blotting

Control (MOCK), GTF2I knockdown cells, and cells which were transfected with GTF2I or its mutants were lysed with lysis buffer (50 mM Tris-HCL [pH 7.4], 150 mM NaCl, 1% Nonidet p-40, and 3 mM EDTA) containing 1/100 volume of protease inhibitor and phosphatase inhibitor cocktails (Sigma Aldrich). SDS-PAGE was subsequently performed, and the proteins were transferred to a polyvinylidene fluoride membrane (Merck Millipore). Immunoblotting was performed according to the manufacturer's protocols.

Luciferase reporter assay

Plasmid vectors encoding GTF2I or its mutant lacking the leucin zipper domain (ΔLZ), pGL4.32 [luc2P/NF-κB-RE/Hygro] (Promega), and pGL4.74 [hRluc/TK] (Promega) were transfected to HEK293T cells with polyethyleneimine. Cells were stimulated for 6 h with the indicated cytokines after 24 h of transfection. The luciferase activities of the total cell lysates were measured using the Dual Luciferase Reporter Assay System (Promega).

Confocal laser scanning microscopy

To show the translocation of p65, Control (MOCK) and GTF2I-knockdown cells were stimulated with TNFα for 0, 15, and 30 min on µ-Slides (Ibidi). To show the intracellular localization of GTF2I, human synoviocytes and HeLa cells were stimulated with or without TNFα. The cells were fixed in 4% paraformaldehyde for 20 min, permeabilized with Perm/Wash solution (Cytofix/Cytoperm Kit, BD Biosciences), and incubated with anti-NF-κB p65 or anti-GTF2I antibody for 1 h. After being washed with Perm/Wash solution, the cells were incubated with anti-rabbit Alexa Fluor 488-conjugated secondary antibody, anti-mouse Alexa Fluor 546-conjugated secondary

antibody, and Hoechst 33342 nuclear stain for 1 h. The cells were then observed by the confocal microscopy LSM5 Pascal system (Carl Zeiss) to assess the translocation of NF-κB p65 to the nucleus.

Immunoprecipitation

Cells were suspended in lysis buffer (50 mM Tris-HCl [pH 7.4], 150 mM NaCl, 1% Nonidet P-40, 3 mM EDTA) and precleared with 30 µl of protein G-sepharose (pharmacia). The supernatant was mixed with 30 µl of FLAG beads (Sigma-Aldrich), followed by rotation for 2 h at 4˚C. For the phosphorylation of NF-κB p65, the supernatant was mixed with 2 µg of anti-NF-κB p65 antibody followed by incubation with rotation overnight at 4˚C. The immunoprecipitate was eluted with FLAG peptide (Sigma Aldrich). The immunoprecipitated samples were boiled in SDS sample buffer for 5 min at 95˚C and used for western blotting.

ChIP assay

Control and GTF2I-knockdown cells were stimulated with TNFα for 60 min. The cells were fixed with 1% PFA and lysed with lysis buffer (10 mM Tris-HCl [pH 7.5], 140 mM NaCl, 1% Triton X-100, 1 mM EDTA, and 1% SDS). The lysate was sonicated to prepare chromatin DNA. Immunoprecipitation was performed with Dynabeads protein G (Life Technologies), and anti-NF-κB p65 antibody, anti-p300 antibody, anti-Pol II antibody, anti-GTF2I antibody or control IgG were added. DNA purification was performed with 10% Chelex 100 (Bio-Rad). Real-time PCR was performed with IL-6, CCL5, and CCL20 promoter primer pairs that included a p65 binding site. The PCR primer sequences are described in Table 3.

RNA sequence analysis

Control and GTF2I-knockdown BC-1 cells were stimulated with TNFα for 3 h. Total RNA was isolated with a TRIzol. cDNAs were synthesized with the NEBNext Ultra RNA Library Prep Kit for Illumina (NEB Biolabs, Inc., Ipswich, MA) according to the manufacturer's instruction. Sequencing data were obtained using the HiSeq 1500 system (Illumina), which could read a 50-bp sequence (single-ended 50-base pair reads). Hierarchical clustering and heat mapping of the data were performed with MeV (http://www.tm4.org/mev/). Data were analyzed with Strand NGS (Strand Genomics).

Statistical analysis

Student's two-tailed *t*-tests were used for the analysis of differences between two groups. One-way analysis of variance with Bonferroni correction was used for multiple comparisons. Wilcoxon’s rank sum test was used for the analysis of clinical scores in the mouse model of arthritis and experiments using enough patient samples ($n>6$). Pearson’s correlation coefficient was used for analyzing correlations between two variables. P values less than 0.05 were considered significant.

Results

GTF2I in nonimmune cells is involved in inflammation responses in vitro and in vivo

We investigated how GTF2I activates the IL-6 amplifier in nonimmune cells. Two GTF2I-knockdown endothelial cells (BC-1 cells) were established by using two lentiviruses with GTF2I shRNAs. The knockdown efficiency was validated by the GTF2I mRNA expression (Figure 1A). IL-6 mRNA expression and protein secretion were suppressed in BC-1 cells with GTF2I-knockdown after IL-6 and IL-17A stimulation (Figures 1B and 1C). Cell viability was not significantly affected by GTF2I-knockdown (Figure 1C). We stimulated BC-1 cells treated with GTF2I shRNA and four TLR ligands and then analyzed the mRNA expressions of IL-6 and Mx1, an interferon-stimulatory gene. We found that GTF2I knockdown suppressed both IL-6 and Mx1 expression by LPS, CpG, and R848 via the TLR-Myd88 pathway, but not by poly (I:C) via the TLR-TRIF pathway (Supplementary Figure 2A and 2B). The knockdown of GTF2I in HSG cells also suppressed the mRNA expression of several inflammatory chemokines such as CCL2, CCL5, CCL20 and CXCL2 after IL-6 and IL-17A stimulation (Figure 1D). Similar results of immune suppression were observed in F759 mice, which developed cytokine-induced arthritis in the ankle joints if treated in the ankle with lentiviruses encoding the GTF2I shRNA (Figure 1E and 1F). Taken together, these results demonstrated that GTF2I in nonimmune cells contributed to the inflammation response in vivo and in vitro.

GTF2I in nonimmune cells is involved in activation of the NF-κB pathway

The IL-6 amplifier is activated by the simultaneous stimulation of NF-κB and STAT3 via inflammatory cytokines in nonimmune cells (5-7,17). GTF2I-knockdown nonimmune cells showed suppressed LCN2 expression, the target gene of the NF-κB pathway, after IL-6 plus IL-17A stimulation, but no inhibition of STAT3, which is the target gene of the STAT3 pathway (Figure 2A). Consistently, the forced expression of GTF2I enhanced NF-κB p65 promoter activity and IL-6 promoter activity (Figure 2B). These results demonstrated that GTF2I in nonimmune cells activates the NF-κB pathway but not the STAT3 pathway.

GTF2I in nonimmune cells is involved in nuclear NF-κB activation by p65 binding

GTF2I translocates to the nucleus in lymphocytes (29-32). We found that GTF2I was also localized in the nucleus regardless of stimulation in nonimmune cells including HeLa cells and human synoviocytes (Figures 2C and 2D). Consistent with these results, cytoplasmic events including the phosphorylation of IκBα and NF-κB p65 and the nuclear translocation of NF-κB p65 were not affected by GTF2I-knockdown after cytokine stimulation (Figure 3A and 3B). On the other hand, the recruitment of NF-κB p65 to the promoter of IL-6 gene was significantly reduced after TNFα stimulation in GTF2I-knockdown nonimmune cells (Figure 3C). Thus, GTF2I in nonimmune cells is involved in nuclear NF-κB activation after cytokine stimulation.

GTF2I is composed of a N-terminal leucine zipper (LZ) domain, two nuclear localizing signals, a basic region, and six repeat domains containing the helix-loop-helix motif (33,34) (Figure 3D). We found GTF2I associated with NF-κB p65 via its LZ domain (Figure 3E). Functionally, deficiency of the LZ domain significantly reduced NF-κB

promoter activity in nonimmune cells (Figure 3F). Together, these results indicated that GTF2I enhances NF-κB activation by p65 binding to its LZ domain in the nucleus of nonimmune cells.

GTF2I in nonimmune cells enhances the recruitment of transcriptional regulators to the promoters of NF-κB target genes

We hypothesized that NF-κB p65 together with GTF2I increases the transcription of NF-κB target genes after cytokine stimulation in nonimmune cells. Consistently, the recruitment of NF-κB p65 was significantly reduced not only to the promoter region of IL-6 (Figure 3C, Supplementary Figure 3A), but also to the promoter regions of CCL2 and CCL5 in GTF2I-knockdown cells after cytokine stimulation (Figure 4A). Moreover, the recruitment of p300 and polymerase II (Pol II) was reduced on the promoter of IL-6 after cytokine stimulation (Figure 4B and 4C). The recruitment of GTF2I itself to the IL-6 promoter increased after cytokine treatment (Figure 4D, Supplementary Figure 3B). Thus, GTF2I enhances the recruitment of transcriptional regulators such as p300 and Pol II to the promoters of NF-κB target genes in nonimmune cells. However, because there were no significant differences between mock or shRNA treated samples after 60-min stimulation (Figure 4B and 4C), we cannot confidently conclude which of p300, Pol II, or GTF2I itself accumulates in the early phase and which accumulates in the late phase.

We then performed ChIP assays on acetyl H3K9 and tri-methyl H3K27 as activation and suppressive markers of histones, respectively, and found that acetyl H3K9 was decreased and tri-methyl H3K27 increased in GTF2I-knockdown cells (Supplementary Figure 4A and 4B). We also found that the mRNA expressions of several histone modificatory enzymes including Gcn5, Hdac2, Ezh2, and Jmjd3 were decreased in GTF2I-knockdown cells (Supplementary Figure 4C). Thus, GTF2I is critical for the epigenetic changes of histones and the expression of histone modificatory enzymes after IL-6 amplifier activation.

We found that GTF2I enhanced p65 binding to the promoters of NF-κB target genes including IL-6 and chemokines after cytokine stimulation (Figure 3C and 4A) and that GTF2I functions at the promoter regions of NF-κB target genes most likely by stabilizing the transcriptional complexes via binding with NF-κB p65 in nonimmune cells (Figure 4B and 4C).

We performed RNA-sequencing experiments using cells with or without GTF2I shRNA in the presence of absence of cytokine stimulation (Figure 5). Figure 5A and 5B show a volcano plot and GO analysis results, respectively. We confirmed that GTF2I is mainly involved in the NF-κB pathway and not the STAT3 pathway, because we found many but not all NF-κB targets were suppressed in cells with GTF2I-knockdown, but the majority of STAT3 targets were unaffected (Figure 5C and 5D). We also show the positions of IL-6, CCL2, CCL5, CCL20, CXCL20, and GTF2I, which are all NF-κB targets, as well as STAT3, which is a STAT3 target (Figure 5C and 5D). Consistently, we confirmed that STAT3 was recruited to the IL-6 promoter, a recruitment dependent on GTF2I (Figure 4D). These results suggest that a specific subset of promoters of NF-κB target genes might be regulated by GTF2I. Additional work is required to identify these adaptor molecules in order to understand more about the inflammation induction in SS.

GTF2I is highly expressed in SS patients having GTF2I SNPs and enhanced activation of the IL-6 amplifier in salivary gland cells

To examine the effect of GTF2I SNPs on GTF2I expression in salivary gland cells, salivary gland samples from SS patients (n = 20) were divided into two groups based on the presence (n = 8) or absence (n = 12) of the risk alleles rs117026326 and rs73366469 (GTF2I SNPs) (Supplementary Figure 1A). No patients expressed the risk alleles of either SNP alone in our cohort (Supplementary Figure 1B). Although we found no significant pathogenic changes between those with or without SNPs based on several criteria including the Greenspan Grade (Table 4), quantification by RT-PCR showed GTF2I expression was significantly higher in salivary glands isolated from SS patients with the risk alleles compared to individuals without (Figure 6A). Moreover, a higher expression of IL-6 and CCL2 was measured in the salivary gland cells of SS patients with the risk alleles (Figure 6B). In agreement with the elevated expressions of IL-6 and CCL2, lymphocyte infiltration levels were also higher (Figure 6C and 6D). IHC of the activation status of NF-κB p65 and STAT3 showed an increase in phosphorylated NF-κB p65 and phosphorylated STAT3 in the salivary gland cells with the risk alleles, and the protein levels of GTF2I were also increased in the salivary gland cells with the risk alleles (Figures 6E and 6F). On the other hand, GTF2I expression, NF-κB activation, and STAT3 activation in immune cells showed no SNP dependency in SS patients (Supplementary Figure 5A and 5B). Thus, the risk alleles of GTF2I SNPs enhance GTF2I expression and activation of the IL-6 amplifier in salivary gland cells, which is critical for the immune cell accumulation.

Discussion

SS, like other autoimmune diseases, is proposed to be initiated by a combination of genetic and environmental factors. Although several studies have investigated changes in gene expressions in the minor salivary glands of SS patients, functional investigations of SNPs identified by GWAS studies have been limited. In this study, we demonstrate that two GTF2I SNPs, rs117026326 and rs73366469, caused an increase in the expressions of GTF2I, IL-6, and chemokines via the activation of NF-κB and STAT3 in salivary gland cells and were associated with lymphocyte infiltration in the salivary glands, most likely via chemokine expression. In agreement, GTF2I overexpression enhanced NF-κB activation, while GTF2I-knockdown decreased chemokine expression even with stimulation by IL-6 and IL17A in nonimmune cells. Thus, GTF2I plays a role in the SS pathogenesis by enhancing NF-κB activation in salivary gland cells.

Other genes located in the same locus as GTF2I may contribute to SS development. Indeed, a fine mapping study reported that the association with SS seen at this locus was most likely explained by a missense variant, p.Arg90H, in the neighbouring NCF1 gene (35). Thus, it is possible that other genes including NCF1 might regulate GTF2I expression indirectly. However, we demonstrated that GTF2I increased in the presence of the risk alleles and that it enhances the activation of the NF-κB pathway in nonimmune cells, which is critical for inflammation development. Thus, we propose that the risk alleles play a role in the development of inflammatory diseases via GTF2I. More study is required to understand how the SNPs increase the expression of GTF2I and also the role of other genes on the pathogenesis.

Importantly, GTF2I mRNA and protein levels were increased in salivary gland cells having the risk alleles compared with samples from non-risk allele patients. Moreover, many salivary gland cells with the risk alleles showed activation of the IL-6 amplifier based on p65 and STAT3 phosphorylation, higher expressions of NF-κB targets such as IL-6 and chemokines, and more infiltration of lymphocytes in the salivary glands. Therefore, we hypothesized that the risk alleles of GTF2I SNPs function in nonimmune cells but not in immune cells of the blood to develop SS. These results suggest GTF2I in salivary gland cells is a key molecule for maintaining the chronic inflammation in SS pathophysiology and is also a potential therapeutic target.

Funding

This work was supported by JSPS KAKENHI (D. K. and M. M.), the Joint Usage/Research Center Institute for Genetic Medicine, Hokkaido University (M. M.), the Photo-excitonix Project at Hokkaido University (M. M.), the Japanese Initiative for Progress of Research on Infectious Disease for Global Epidemic (M. M.), the Takeda Science Foundation (M. M.), the Institute for Fermentation Osaka (M. M.), Mitsubishi Foundation (M. M.), Uehara Memorial Foundation (M. M.), and Tokyo Biomedical Research Foundation (M. M.). This study was supported by an NIDCR, NIH intramural research grant to JAC (1ZIADE000695).

Acknowledgements

The authors acknowledge Prof. Yoshimasa Kitagawa and Dr. Emi Yamashita (Oral Diagnosis and Medicine, Department of Oral Pathobiological Science, Hokkaido University, Japan) for performing the labial gland biopsies. We also thank Prof. Takayuki Sumida and Dr. Hiroto Tsuboi for providing the salivary gland tissues of SS patients. We thank Dr P. Karagiannis (CiRA, Kyoto University, Kyoto, Japan) for carefully reading the manuscript and important discussion. We are grateful to Ms. Chiemi Nakayama, Ms. Mitsue Ezawa, and Ms. Satomi Fukumoto for excellent administrative assistance.

Author contributions

All authors were involved in drafting the article or revising it critically for important intellectual content, and all authors approved the final version to be published.

Study conception and design, DK and MM; manuscript writing, SS, IN, DK and MM; acquisition of data, SS, IN, YT, TA, JJJ and DK; analysis and interpretation of data, SS, IN, JJJ, YT, JAC, TA, YH, OO, DK, and MM; provision of human samples, TA and IM.

Competing interests

The authors have no conflict of interests to be disclosed.

Reference

1 Singh, N. and Cohen, P. L. 2012. The T cell in Sjogren's syndrome: force majeure, not spectateur. *J. Autoimmun.* 39:229.

2 Verstappen, G. M., Corneth, O. B. J., Bootsma, H., and Kroese, F. G. M. 2018. Th17 cells in primary Sjogren's syndrome: Pathogenicity and plasticity. *J. Autoimmun.* 87:16.

3 Lee, S. Y., Han, S. J., Nam, S. M., Yoon, S. C., Ahn, J. M., Kim, T. I., Kim, E. K., and Seo, K. Y. 2013. Analysis of tear cytokines and clinical correlations in Sjogren syndrome dry eye patients and non-Sjogren syndrome dry eye patients. *Am. J. Ophthalmol.* 156:247.

4 Katsifis, G. E., Rekka, S., Moutsopoulos, N. M., Pillemer, S., and Wahl, S. M. 2009. Systemic and local interleukin-17 and linked cytokines associated with Sjogren's syndrome immunopathogenesis. *Am. J. Pathol.* 175:1167.

5 Murakami, M., Kamimura, D., and Hirano, T. 2019. Pleiotropy and Specificity: Insights from the Interleukin 6 Family of Cytokines. *Immunity* 50:812.

6 Ogura, H., Murakami, M., Okuyama, Y., Tsuruoka, M., Kitabayashi, C., Kanamoto, M., Nishihara, M., Iwakura, Y., and Hirano, T. 2008. Interleukin-17 promotes autoimmunity by triggering a positive-feedback loop via interleukin-6 induction. *Immunity* 29:628.

7 Atsumi, T., Singh, R., Sabharwal, L., Bando, H., Meng, J., Arima, Y., Yamada, M., Harada, M., Jiang, J. J., Kamimura, D., Ogura, H., Hirano, T., and Murakami, M. 2014. Inflammation amplifier, a new paradigm in cancer biology. *Cancer Res.* 74:8.

8 Tanaka, H., Arima, Y., Kamimura, D., Tanaka, Y., Takahashi, N., Uehata, T., Maeda, K., Satoh, T., Murakami, M., and Akira, S. 2019. Phosphorylation-dependent Regnase-1 release from endoplasmic reticulum is critical in IL-17 response. *J. Exp. Med.* 216:1431.

9 Stofkova, A., Kamimura, D., Ohki, T., Ota, M., Arima, Y., and Murakami, M. 2019. Photopic light-mediated down-regulation of local alpha1A-adrenergic signaling protects blood-retina barrier in experimental autoimmune uveoretinitis. *Sci. Rep.* 9:2353.

10 Ota, M., Tanaka, Y., Nakagawa, I., Jiang, J. J., Arima, Y., Kamimura, D., Onodera, T., Iwasaki, N., and Murakami, M. 2019. Role of Chondrocytes in the Development of Rheumatoid Arthritis Via Transmembrane Protein 147-Mediated NF-kappaB Activation. *Arthritis Rheumatol.*

11 Fujita, M., Yamamoto, Y., Jiang, J. J., Atsumi, T., Tanaka, Y., Ohki, T., Murao, N., Funayama, E., Hayashi, T., Osawa, M., Maeda, T., Kamimura, D., and Murakami, M. 2019. NEDD4 Is Involved in Inflammation Development during Keloid Formation. *J. Invest. Dermatol.* 139:333.

12 Tanaka, Y., Sabharwal, L., Ota, M., Nakagawa, I., Jiang, J. J., Arima, Y., Ogura, H., Okochi, M., Ishii, M., Kamimura, D., and Murakami, M. 2018. Presenilin 1 Regulates NF-kappaB Activation via Association with Breakpoint Cluster Region and Casein Kinase II. *J. Immunol.* 201:2256.

13 Okuyama, Y., Tanaka, Y., Jiang, J. J., Kamimura, D., Nakamura, A., Ota, M., Ohki, T.,

Higo, D., Ogura, H., Ishii, N., Atsumi, T., and Murakami, M. 2018. Bmi1 Regulates IkappaBalpha Degradation via Association with the SCF Complex. *J. Immunol.* 201:2264.

14 Atsumi, T., Suzuki, H., Jiang, J. J., Okuyama, Y., Nakagawa, I., Ota, M., Tanaka, Y., Ohki, T., Katsunuma, K., Nakajima, K., Hasegawa, Y., Ohara, O., Ogura, H., Arima, Y., Kamimura, D., and Murakami, M. 2017. Rbm10 regulates inflammation development via alternative splicing of Dnmt3b. *Int. Immunol.* 29:581.

15 Arima, Y., Ohki, T., Nishikawa, N., Higuchi, K., Ota, M., Tanaka, Y., Nio-Kobayashi, J., Elfeky, M., Sakai, R., Mori, Y., Kawamoto, T., Stofkova, A., Sakashita, Y., Morimoto, Y., Kuwatani, M., Iwanaga, T., Yoshioka, Y., Sakamoto, N., Yoshimura, A., Takiguchi, M., Sakoda, S., Prinz, M., Kamimura, D., and Murakami, M. 2017. Brain micro-inflammation at specific vessels dysregulates organ-homeostasis via the activation of a new neural circuit. *Elife* 6.

16 Meng, J., Jiang, J. J., Atsumi, T., Bando, H., Okuyama, Y., Sabharwal, L., Nakagawa, I., Higuchi, H., Ota, M., Okawara, M., Ishitani, R., Nureki, O., Higo, D., Arima, Y., Ogura, H., Kamimura, D., and Murakami, M. 2016. Breakpoint Cluster Region-Mediated Inflammation Is Dependent on Casein Kinase II. *J. Immunol.* 197:3111.

17 Nakagawa, I., Kamimura, D., Atsumi, T., Arima, Y., and Murakami, M. 2015. Role of Inflammation Amplifier-Induced Growth Factor Expression in the Development of Inflammatory Diseases. *Crit. Rev. Immunol.* 35:365.

18 Murakami, M., Harada, M., Kamimura, D., Ogura, H., Okuyama, Y., Kumai, N., Okuyama, A., Singh, R., Jiang, J. J., Atsumi, T., Shiraya, S., Nakatsuji, Y., Kinoshita, M., Kohsaka, H., Nishida, M., Sakoda, S., Miyasaka, N., Yamauchi-Takihara, K., and Hirano, T. 2013. Disease-association analysis of an inflammation-related feedback loop. *Cell Rep* 3:946.

19 Lee, J., Nakagiri, T., Oto, T., Harada, M., Morii, E., Shintani, Y., Inoue, M., Iwakura, Y., Miyoshi, S., Okumura, M., Hirano, T., and Murakami, M. 2012. IL-6 amplifier, NF-kappaB-triggered positive feedback for IL-6 signaling, in grafts is involved in allogeneic rejection responses. *J. Immunol.* 189:1928.

20 Arima, Y., Harada, M., Kamimura, D., Park, J. H., Kawano, F., Yull, F. E., Kawamoto, T., Iwakura, Y., Betz, U. A., Marquez, G., Blackwell, T. S., Ohira, Y., Hirano, T., and Murakami, M. 2012. Regional neural activation defines a gateway for autoreactive T cells to cross the blood-brain barrier. *Cell* 148:447.

21 Murakami, M., Okuyama, Y., Ogura, H., Asano, S., Arima, Y., Tsuruoka, M., Harada, M., Kanamoto, M., Sawa, Y., Iwakura, Y., Takatsu, K., Kamimura, D., and Hirano, T. 2011. Local microbleeding facilitates IL-6- and IL-17-dependent arthritis in the absence of tissue antigen recognition by activated T cells. *J. Exp. Med.* 208:103.

22 Takada, Y., Kamimura, D., Jiang, J. J., Higuchi, H., Iwami, D., Hotta, K., Tanaka, Y., Ota, M., Higuchi, M., Nishio, S., Atsumi, T., Shinohara, N., Matsuno, Y., Tsuji, T., Tanabe,

T., Sasaki, H., Iwahara, N., and Murakami, M. 2020. Increased urinary exosomal SYT17 levels in chronic active antibody-mediated rejection after kidney transplantation via the IL-6 amplifier. *Int. Immunol.*

23 Higuchi, H., Kamimura, D., Jiang, J. J., Atsumi, T., Iwami, D., Hotta, K., Harada, H., Takada, Y., Kanno-Okada, H., Hatanaka, K. C., Tanaka, Y., Shinohara, N., and Murakami, M. 2020. Orosomucoid 1 is involved in the development of chronic allograft rejection after kidney transplantation. *Int. Immunol.*

24 Fang, K., Zhang, K., and Wang, J. 2015. Network-assisted analysis of primary Sjogren's syndrome GWAS data in Han Chinese. *Sci. Rep.* 5:18855.

25 Li, Y., Zhang, K., Chen, H., Sun, F., Xu, J., Wu, Z., Li, P., Zhang, L., Du, Y., Luan, H., Li, X., Wu, L., Li, H., Wu, H., Li, X., Li, X., Zhang, X., Gong, L., Dai, L., Sun, L., Zuo, X., Xu, J., Gong, H., Li, Z., Tong, S., Wu, M., Li, X., Xiao, W., Wang, G., Zhu, P., Shen, M., Liu, S., Zhao, D., Liu, W., Wang, Y., Huang, C., Jiang, Q., Liu, G., Liu, B., Hu, S., Zhang, W., Zhang, Z., You, X., Li, M., Hao, W., Zhao, C., Leng, X., Bi, L., Wang, Y., Zhang, F., Shi, Q., Qi, W., Zhang, X., Jia, Y., Su, J., Li, Q., Hou, Y., Wu, Q., Xu, D., Zheng, W., Zhang, M., Wang, Q., Fei, Y., Zhang, X., Li, J., Jiang, Y., Tian, X., Zhao, L., Wang, L., Zhou, B., Li, Y., Zhao, Y., Zeng, X., Ott, J., Wang, J., and Zhang, F. 2013. A genome-wide association study in Han Chinese identifies a susceptibility locus for primary Sjogren's syndrome at 7q11.23. *Nat. Genet.* 45:1361.

26 Sun, C., Molineros, J. E., Looger, L. L., Zhou, X. J., Kim, K., Okada, Y., Ma, J., Qi, Y. Y., Kim-Howard, X., Motghare, P., Bhattarai, K., Adler, A., Bang, S. Y., Lee, H. S., Kim, T. H., Kang, Y. M., Suh, C. H., Chung, W. T., Park, Y. B., Choe, J. Y., Shim, S. C., Kochi, Y., Suzuki, A., Kubo, M., Sumida, T., Yamamoto, K., Lee, S. S., Kim, Y. J., Han, B. G., Dozmorov, M., Kaufman, K. M., Wren, J. D., Harley, J. B., Shen, N., Chua, K. H., Zhang, H., Bae, S. C., and Nath, S. K. 2016. High-density genotyping of immune-related loci identifies new SLE risk variants in individuals with Asian ancestry. *Nat. Genet.* 48:323.

27 Teos, L. Y. and Alevizos, I. 2017. Genetics of Sjogren's syndrome. *Clin. Immunol.* 182:41.

28 Shiboski, C. H., Shiboski, S. C., Seror, R., Criswell, L. A., Labetoulle, M., Lietman, T. M., Rasmussen, A., Scofield, H., Vitali, C., Bowman, S. J., Mariette, X., and International Sjogren's Syndrome Criteria Working, G. 2017. 2016 American College of Rheumatology/European League Against Rheumatism classification criteria for primary Sjogren's syndrome: A consensus and data-driven methodology involving three international patient cohorts. *Ann. Rheum. Dis.* 76:9.

29 Cheriyath, V., Desgranges, Z. P., and Roy, A. L. 2002. c-Src-dependent transcriptional activation of TFII-I. *J. Biol. Chem.* 277:22798.

30 Novina, C. D., Cheriyath, V., and Roy, A. L. 1998. Regulation of TFII-I activity by phosphorylation. *J. Biol. Chem.* 273:33443.

31 Novina, C. D., Kumar, S., Bajpai, U., Cheriyath, V., Zhang, K., Pillai, S., Wortis, H. H.,

and Roy, A. L. 1999. Regulation of nuclear localization and transcriptional activity of TFII-I by Bruton's tyrosine kinase. *Mol. Cell. Biol.* 19:5014.

32 Yang, W. and Desiderio, S. 1997. BAP-135, a target for Bruton's tyrosine kinase in response to B cell receptor engagement. *Proc. Natl. Acad. Sci. U. S. A.* 94:604.

33 Roy, A. L. 2001. Biochemistry and biology of the inducible multifunctional transcription factor TFII-I. *Gene* 274:1.

34 Roy, A. L., Du, H., Gregor, P. D., Novina, C. D., Martinez, E., and Roeder, R. G. 1997. Cloning of an inr- and E-box-binding protein, TFII-I, that interacts physically and functionally with USF1. *EMBO J.* 16:7091.

35 Zhao, J., Ma, J., Deng, Y., Kelly, J. A., Kim, K., Bang, S. Y., Lee, H. S., Li, Q. Z., Wakeland, E. K., Qiu, R., Liu, M., Guo, J., Li, Z., Tan, W., Rasmussen, A., Lessard, C. J., Sivils, K. L., Hahn, B. H., Grossman, J. M., Kamen, D. L., Gilkeson, G. S., Bae, S. C., Gaffney, P. M., Shen, N., and Tsao, B. P. 2017. A missense variant in NCF1 is associated with susceptibility to multiple autoimmune diseases. *Nat. Genet.* 49:433.

Figure 1. GTF2I in nonimmune cells is involved in inflammation induction in vitro and in vivo

(A-B) Mouse BC-1 cells were transduced with lentiviruses that encoded shRNA specific for GTF2I or a control. GTF2I-knockdown cells were stimulated with human IL-6 plus soluble IL-6R and/or IL-17A for 3 h. The mRNA expressions of GTF2I (A) and IL-6 (B) were measured.

(C) GTF2I-knockdown cells were treated with IL-6 plus soluble IL-6R and/or IL-17A for 24 h. The culture supernatant was collected and assessed with ELISA specific for mouse IL-6. Cell survival was also evaluated based on mitochondrial activity using TCO reagent (closed squares).

(D) Human HeLa cells were treated with siRNA specific for GTF2I (si-GTF2I) or control. The knockdown efficiency of GTF2I mRNA levels was assessed. The mRNA expressions of several inflammatory chemokines (CXCL2, CCL2, CCL5, CCL20) were measured.

(E) The knockdown efficiency of GTF2I mRNA levels in F759 mice ankle joints was assessed (n=3, each group).

(F) Clinical arthritis scores from the hind limb of F759 mice after the injection of a lentivirus carrying GTF2I shRNA (gtf2i sh1 or gtf2i sh2) or a control lentivirus (NTC) to the ankle joint on days 0, 2, and 4, and the subsequent administration of IL-6 and IL-17 on days 5, 7, and 9.

Mean scores ± SEM are shown. Data are representative of three independent experiments, each with four subjects. *p<0.05, ** p <0.01, *** p <0.001.

Figure 2. GTF2I is involved in activation of the NF-κB pathway in nonimmune cells.

(A) GTF2I-knockdown BC-1 cells were stimulated with IL-6 plus IL-6R and IL-17A, and the mRNA expressions of LCN2 (left) and STAT3 (right) were measured.

(B) Luciferase assay using NF-κB p65 binding sites (left) or the IL-6 promoter (right) in HEK 293T cells with or without GTF2I overexpression in the presence or absence of TNFα stimulation.

(C,D) HSG cells (C) and human synoviocytes (D) were stimulated with TNFα, and the localization of GTF2I (red) and NF-κB p65 (green) was investigated.

Mean scores ± SEM are shown. Data are representative of three independent experiments, each with four or six subjects. *p<0.05, ** p <0.01, *** p <0.001.

Figure 3. GTF2I in nonimmune cells is involved in nuclear NF-κB activation by p65 binding

(A) GTF2I-knockdown and control cells were treated with TNFα. Phosphorylated NF-κBp65, phosphorylated IκBα, IκBα, GTF2I, and tubulin levels were measured.

(B) GTF2I-knockdown and control cells were stimulated with TNFα, and the cellular localization of NF-κB p65 (red) was observed. Nuclear counterstaining was performed (blue). The bar graph shows the percentages of cells with NF-κB p65 localized in the cytoplasm or the nucleus.

(C) NF-κB p65 recruitment to the IL-6 promoter with TNFα was assessed using ChIP assays in MOCK and GTF2I-knockdown cells.
(D) Schematic illustration of GTF2I proteins. BR, basic region; C, C-terminus; LZ, leucine zipper; N, N-terminus; NLS, nuclear localizing signal; R1-R6, helix-loop-helix motifs.
(E) Plasmids encoding wild-type GTF2I, GTF2I DLZ, or mock vector were transfected. Whole cell lysates were immunoprecipitated with anti-FLAG Ab and p65 Ab, followed by immunoblot analysis with anti-FLAG and anti-NF-κB p65 antibodies.
(F) NF-κB promoter activity in HEK293T cells transfected as in (D) was assessed in the presence of TNFα stimulation.
Mean scores ± SEM are shown. Data are representative of three independent experiments, each with four subjects. ** p <0.01, *** p <0.001.

Figure 4. GTF2I enhances the recruitment of transcriptional regulators to NF-κB promoters in nonimmune cells.
(A) NF-κB p65 recruitment to CCL2 and CCL5 promoters with or without 180 min of IL-6 and IL-17 stimulation was assessed using ChIP assays in MOCK and GTF2I-knockdown cells (sh1 and sh2).
(B) P300 recruitment to the IL-6 promotor with 0, 60, 120, or 180 min of IL-6 and IL-17 stimulation was assessed using ChIP assays in MOCK and GTF2I-knockdown cells.
(C) Pol II recruitment to the IL-6 promotor with 0, 60, 120, or 180 min of IL-6 and IL-17 stimulation was assessed using ChIP assays in MOCK and GTF2I-knockdown cells.
(D) STAT3 recruitment to the IL-6 promotor with 0, 60, 120, or 180 min of IL-6 and IL-17 stimulation was assessed using ChIP assays in MOCK and GTF2I-knockdown cells.
Mean scores ± SEM are shown. Data are representative of three independent experiments, each with four subjects. *p<0.05; ** p <0.01; *** p <0.001.

Figure 5. A specific subset of NF-κB target genes is regulated by GTF2I.
(A) Results of RNA-sequencing data from GTF2I-knockdown and control BC-1 cells. Log Fold changes >1 or <-1 were considered significant.
(B) Down-regulated pathways in GTF2I-knockdown BC-1 cells according to Gene Ontology enrichment analysis.
(C) Scatter plot of p65 target gene expressions based on the RNA-sequencing data from GTF2I-knockdown and control BC-1 cells. The x-axis is the log2 fold change of GTF2I-knockdown cells. The y-axis is the log2 fold change of IL-6 and IL-17 stimulation.
(D) Scatter plot of STAT3 target gene expressions based on the RNA sequence data from GTF2I-knockdown and control BC-1 cells. The axes are the same as in (C).

Figure 6. GTF2I enhanced the activation of NF-κB p65 and STAT3 in salivary gland cells.

(A) GTF2I mRNA levels in the salivary glands of SS patients with (SNP +) or without (SNP -) the risk loci of the GTF2I SNPs are shown as relative expression levels to GAPDH. GTF2I risk SNPs were evaluated by using salivary gland RNA from 20 SS patients at Tsukuba University Hospital.
(B) The mRNA levels of IL-6 and CCl2 in the salivary glands of the same SS patients are shown as relative expression levels to GAPDH.
(C) Hematoxylin and eosin staining were performed in the salivary glands of the same SS patients. Lymphocyte infiltration in the salivary glands is shown. Scale bars, 100 μm.
(D) Quantification of (C) using image J software.
(E) Serial sections of salivary glands from healthy donors and patients at Hokkaido University Hospital with or without the risk alleles were stained with anti-GTF2I antibody, anti-phospho-NF-κB p65 antibody, and anti-phospho-STAT3 antibody. Scale bars, 10 μm.
(F) Quantification of (E) using Image J software.

Median ± interquartile ranges in (A) and (B) or mean scores ± SEM in (D) and (F) are shown. *p < 0.05; **p<0.01.

Supplementary Figure 1. GTF2I SNPs and SS samples

(A) Schematic illustration of the location of the SNPs (rs73366469 and rs117026326) and GTF2I, GTF2IRD1 and GTF2IRD2 genes in chromosome 7.

(B) Genotypes of the two SNPs in SS samples. Heterozygotes and homozygotes of the risk locus are indicated by ± and +, respectively.

Supplementary Figure 2. GTF2I in nonimmune cells is involved in Toll-like receptor-induced inflammation in vitro

(A-B) GTF2I-knockdown BC-1 cells were stimulated with LPS, poly (I:C), CpG, or R848 for 3 h. The mRNA expressions of IL-6 (A) and Mx-1 (B) were measured.

Mean scores ± SEM are shown. Data are representative of three independent experiments, each with three subjects. *p<0.05, ** p <0.01, *** p <0.001.

Supplementary Figure 3. GTF2I enhances the recruitment of transcriptional regulators to NF-κB promoters in salivary gland cells.

(A) NF-κB p65 recruitment to the IL-6 promoter after 0, 60, 120 or 180 min of IL-6 and IL-17 stimulation was assessed using ChIP assays in MOCK and GTF2I-knockdown HSG cells 24 hr after siRNA administration.

(B) GTF2I recruitment to the IL-6 promoter after 0, 60, 120 or 180 min of IL-6 and IL-17 stimulation was assessed using ChIP assays in HSG cells.

Mean scores ± SEM are shown. Data are representative of two independent experiments, each with three subjects. *p<0.05, ** p <0.01.

Supplementary Figure 4. GTF2I induces epigenetic change through histone modulator expression.

(A-B) Acetyl H3K9 recruitment (A) and tri-methyl H3K27 recruitment (B) to the IL-6 promotor with or without 180 min of IL-6 and IL-17 stimulation was assessed using ChIP assays in MOCK and GTF2I-knockdown cells.
(C) The mRNA expressions of a H3K9 acetyltransferase (*Gcn5*), a histone deacetylase (Hdac2), a H3K27 N-methyltransferase (Ezh2), and a histone H3K27 demethylase (Jmjd3) were assessed in MOCK and GTF2I-knockdown cells.
Mean scores ± SEM are shown. Data are representative of three independent experiments, each with three or four subjects. *p<0.05, ** p <0.01, *** p <0.001.

Supplementary Figure 5. GTF2I contribution to the activation of NF-κB p65 and STAT3 in salivary gland cells and infiltrating immune cells.
(A) Representative images of GTF2I, phospho-p65, and phospho-STAT3 intensity in infiltrating immune cells in SS salivary glands with SNPs. Scale bars, 10 μm.
(B) The percentage of immune cells positive for GTF2I, phospho-p65, and phospho-STAT3 and infiltrating the salivary glands tissue from patients with or without SNPs at Hokkaido University Hospital.
Mean ± SEM are shown. NS, not significant.

Figure 1

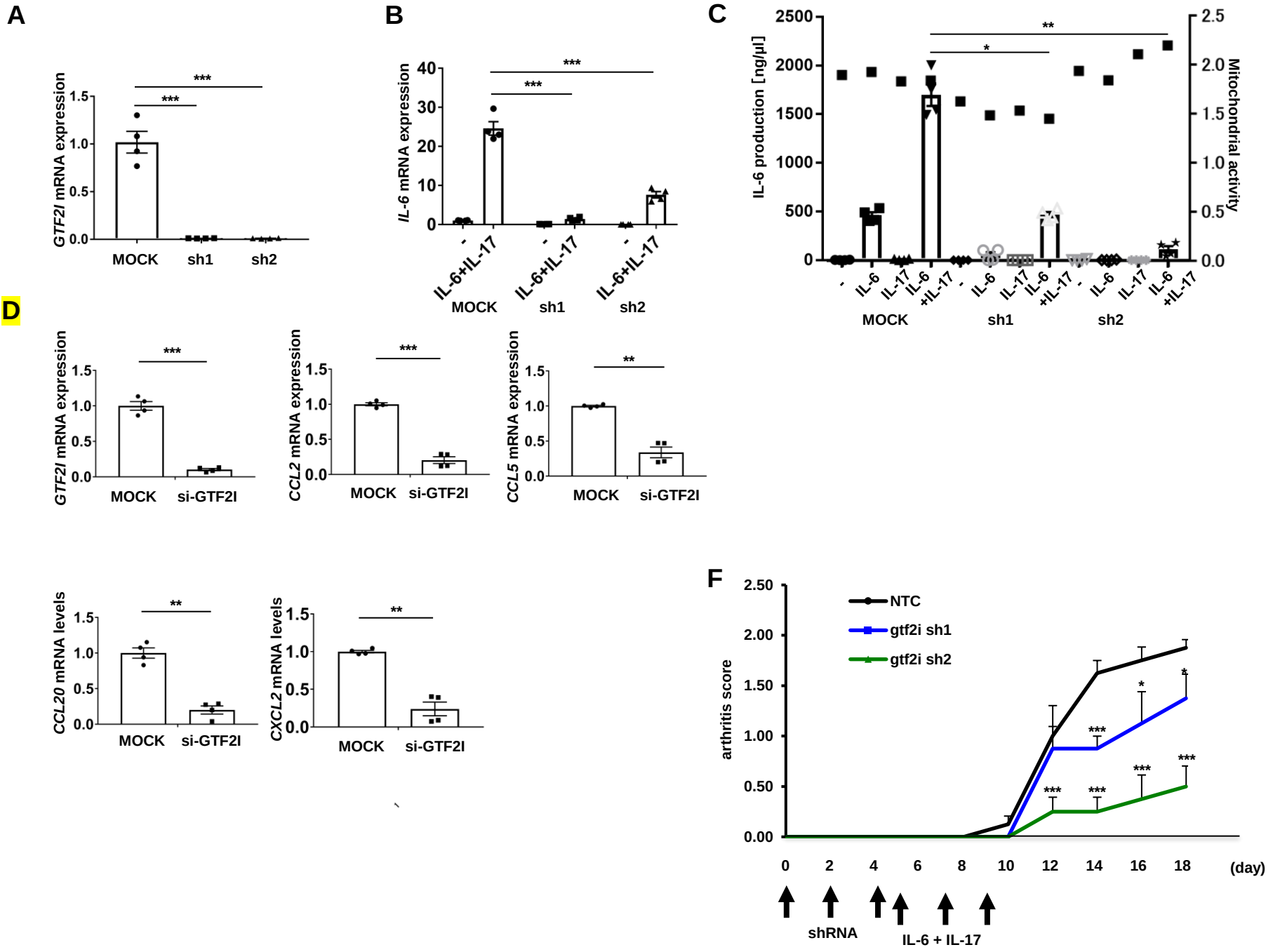
A
GTF2I mRNA expression
MOCK
sh1
sh2
B
IL-6 mRNA expression
IL-6+IL-17
MOCK
sh1
sh2
C
IL-6 production [ng/μl]
Mitochondrial activity
MOCK
sh1
sh2
D
GTF2I mRNA expression
CCL2 mRNA expression
CCL5 mRNA expression
CCL20 mRNA levels
CXCL2 mRNA levels
MOCK
si-GTF2I
F
NTC
gtf2i sh1
gtf2i sh2
arthritis score
(day)
shRNA
IL-6 + IL-17

Figure 2

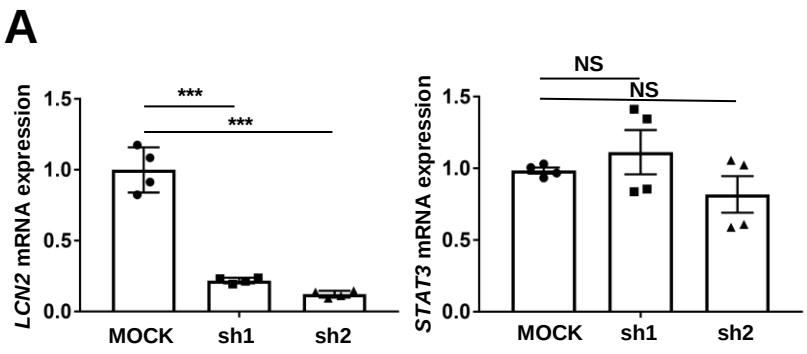
A
LCN2 mRNA expression
1.5
1.0
0.5
0.0
***
***
MOCK
sh1
sh2
STAT3 mRNA expression
NS
NS
MOCK
sh1
sh2

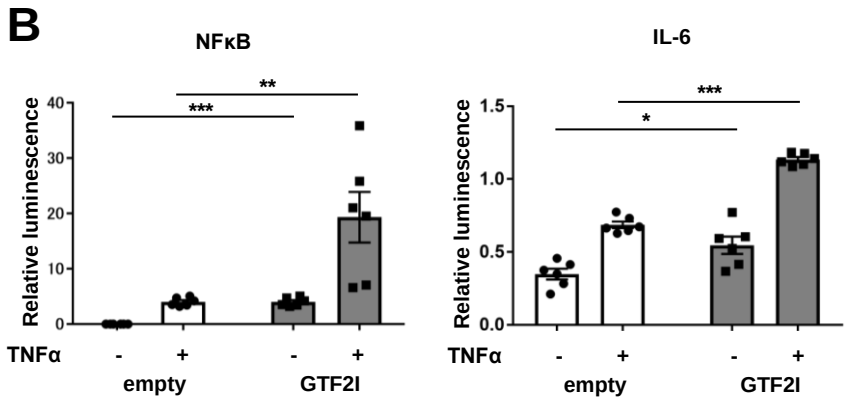
B
NFκB
Relative luminescence
40
30
20
10
0
**
***
TNFα
-
+
-
+
empty
GTF2I
IL-6
Relative luminescence
1.5
1.0
0.5
0.0
***
*
TNFα
-
+
-
+
empty
GTF2I

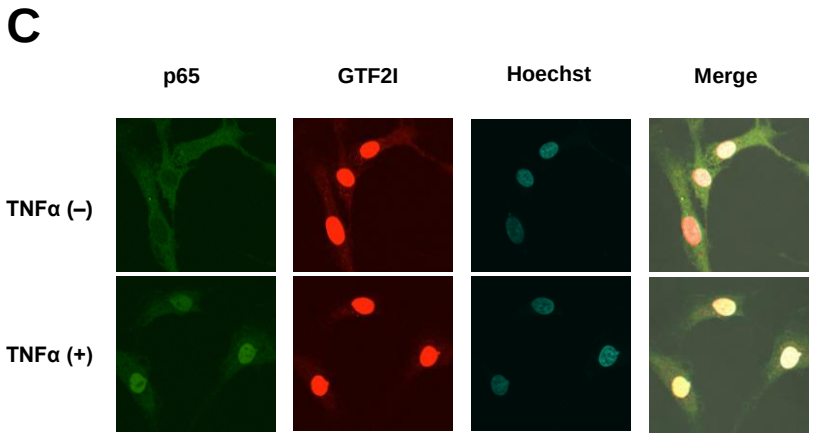
C
p65
GTF2I
Hoechst
Merge
TNFα (–)
TNFα (+)

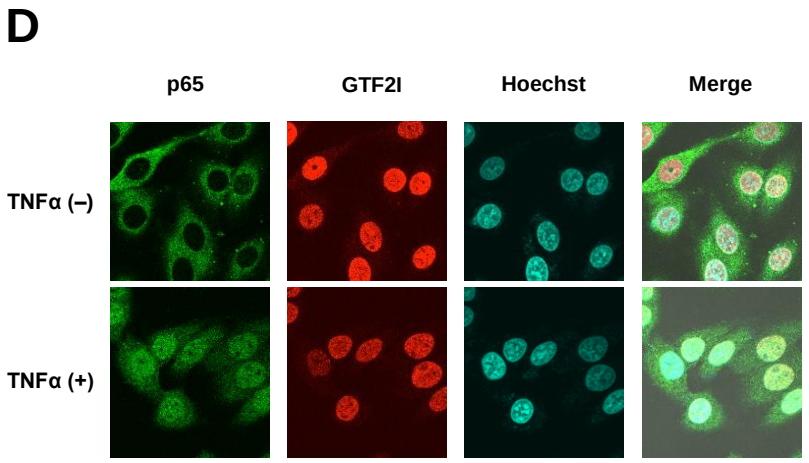
D
p65
GTF2I
Hoechst
Merge
TNFα (–)
TNFα (+)

Figure 3

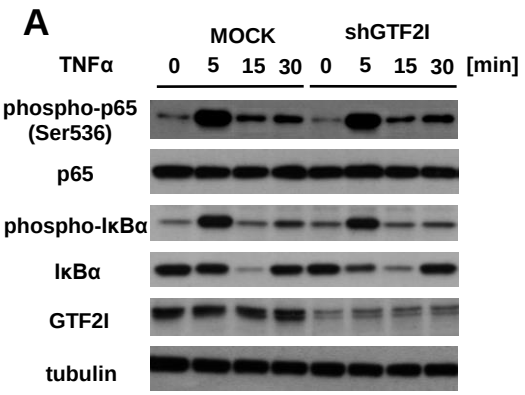
A
MOCK
shGTF2I
TNFα
0 5 15 30 0 5 15 30 [min]
phospho-p65 (Ser536)
p65
phospho-IκBα
IκBα
GTF2I
tubulin

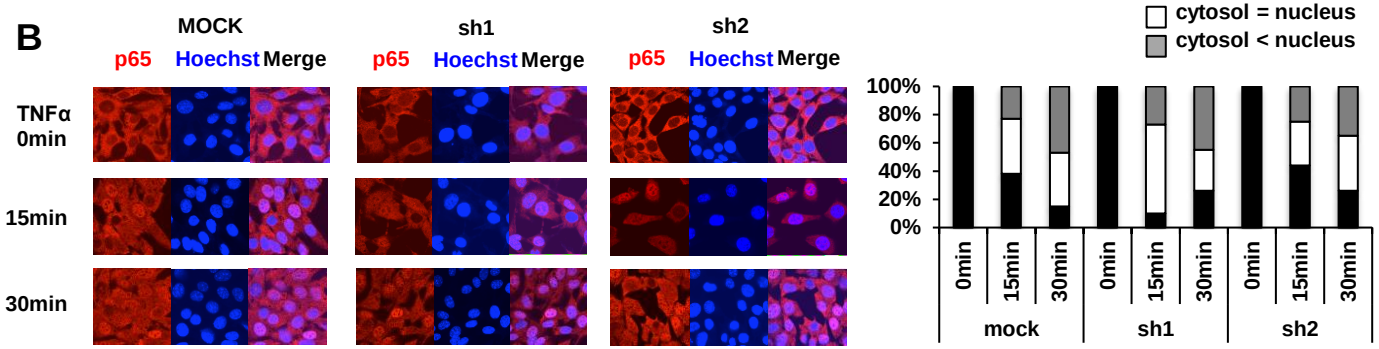
B
MOCK
sh1
sh2
p65 Hoechst Merge
TNFα 0min
15min
30min
cytosol > nucleus
cytosol = nucleus
cytosol < nucleus
100%
80%
60%
40%
20%
0%
0min 15min 30min 0min 15min 30min 0min 15min 30min
mock
sh1
sh2

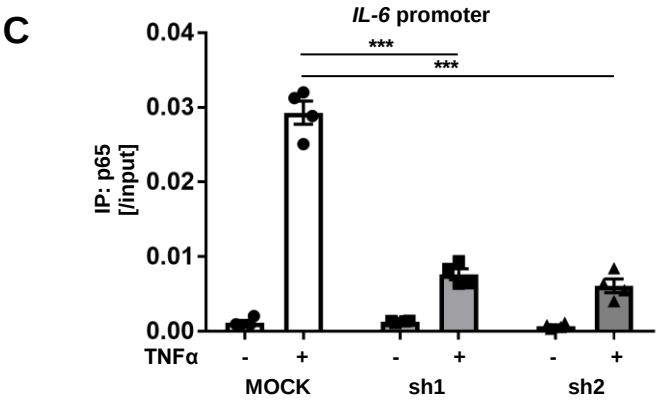
C
IL-6 promoter
IP: p65 [/input]
0.04
0.03
0.02
0.01
0.00
***
***
TNFα - + - + - +
MOCK
sh1
sh2

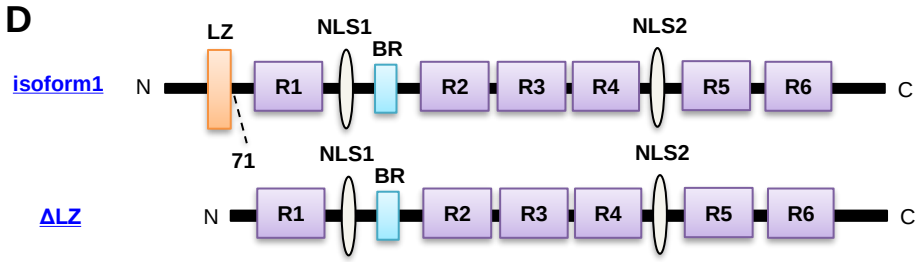
D
isoform1
N
LZ
NLS1
BR
NLS2
R1
R2
R3
R4
R5
R6
C
71
ΔLZ

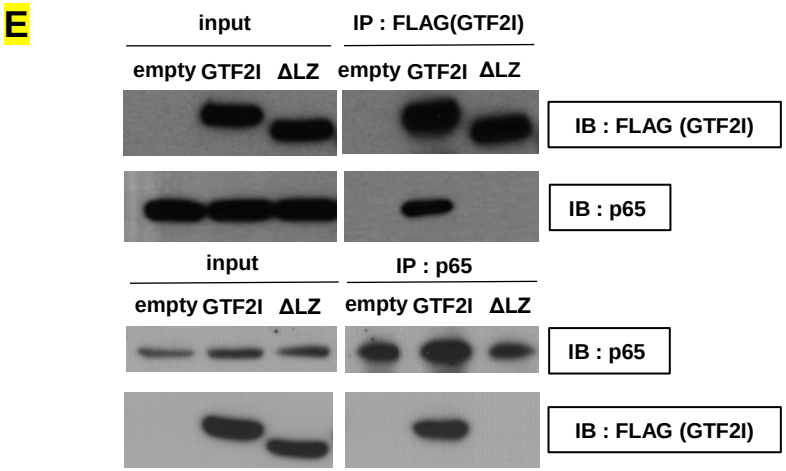
E
input
IP : FLAG(GTF2I)
empty GTF2I ΔLZ
empty GTF2I ΔLZ
IB : FLAG (GTF2I)
IB : p65
input
IP : p65
empty GTF2I ΔLZ
empty GTF2I ΔLZ
IB : p65
IB : FLAG (GTF2I)

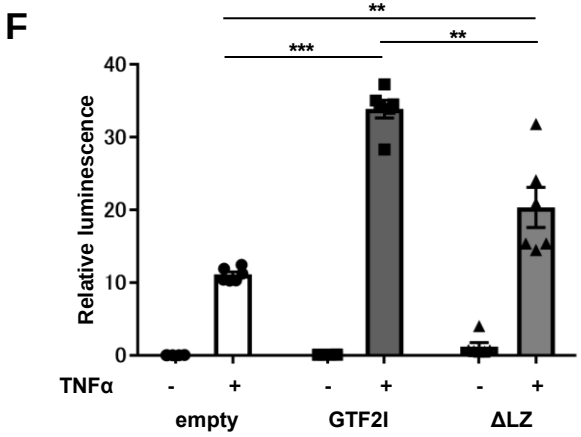
F
Relative luminescence
40
30
20
10
0
**
***
**
TNFα - + - + - +
empty
GTF2I
ΔLZ

Figure 4

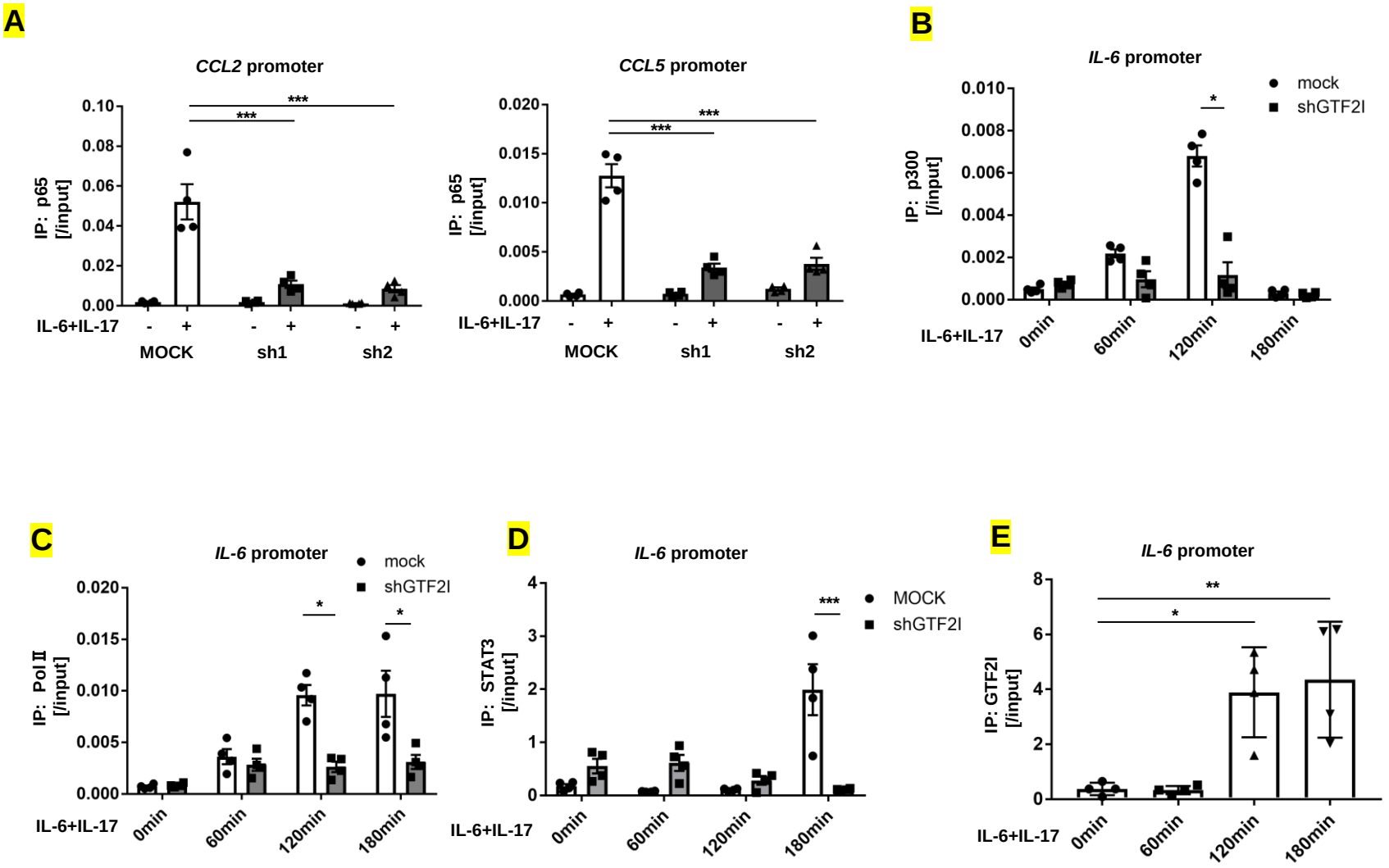
A
CCL2 promoter
IP: p65 [/input]
0.10
0.08
0.06
0.04
0.02
0.00
***
***
IL-6+IL-17
- + - + - +
MOCK sh1 sh2
CCL5 promoter
IP: p65 [/input]
0.020
0.015
0.010
0.005
0.000
***
***
IL-6+IL-17
- + - + - +
MOCK sh1 sh2
B
IL-6 promoter
IP: p300 [/input]
0.010
0.008
0.006
0.004
0.002
0.000
*
mock
shGTF2I
IL-6+IL-17
0min 60min 120min 180min
C
IL-6 promoter
IP: Pol II [/input]
0.020
0.015
0.010
0.005
0.000
*
*
mock
shGTF2I
IL-6+IL-17
0min 60min 120min 180min
D
IL-6 promoter
IP: STAT3 [/input]
4
3
2
1
0
***
MOCK
shGTF2I
IL-6+IL-17
0min 60min 120min 180min
E
IL-6 promoter
IP: GTF2I [/input]
8
6
4
2
0
**
*
IL-6+IL-17
0min 60min 120min 180min

Figure 5

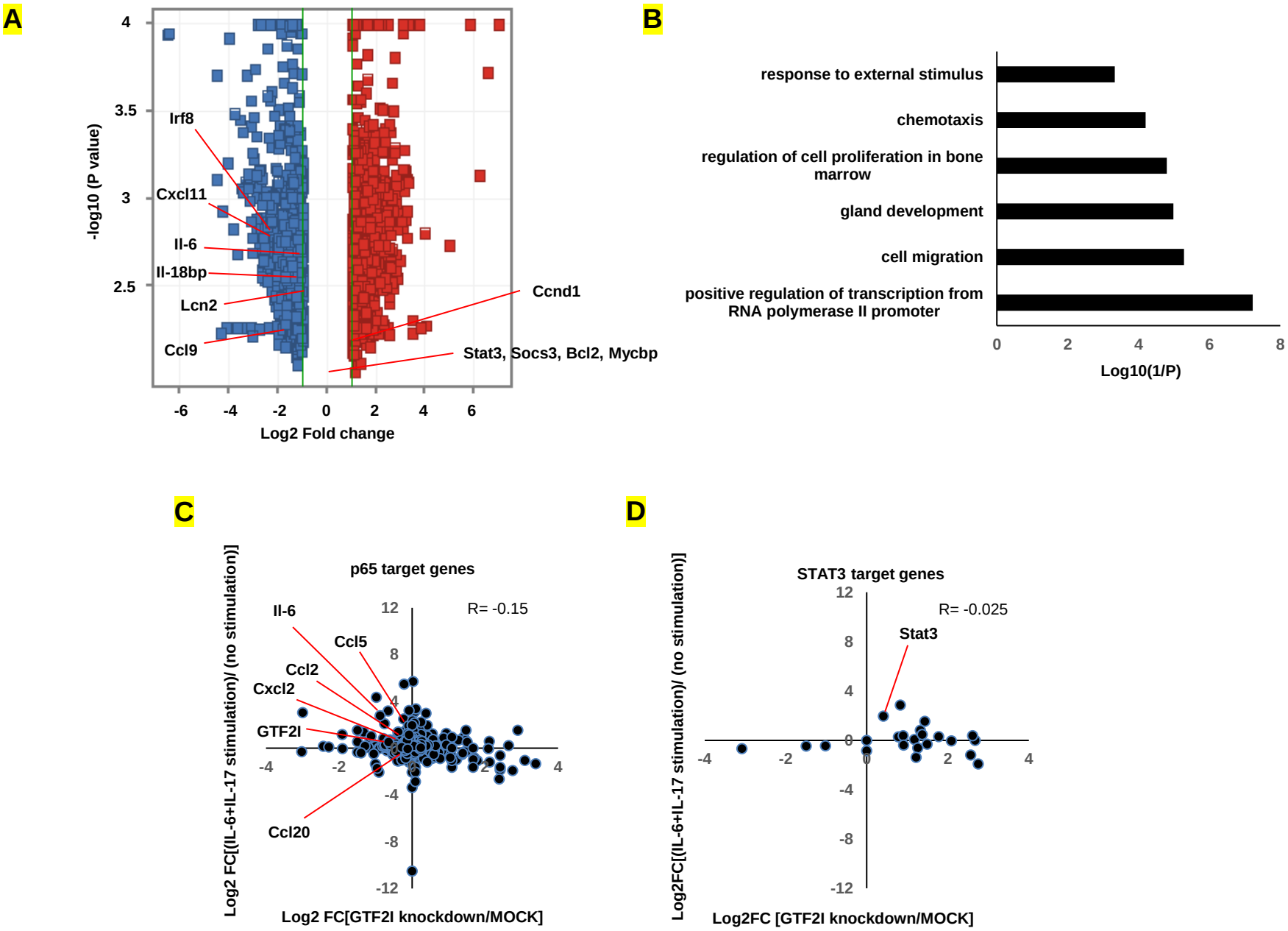
A
-log10 (P value)
Log2 Fold change
Irf8
Cxcl11
Il-6
Il-18bp
Lcn2
Ccl9
Ccnd1
Stat3, Socs3, Bcl2, Mycbp
B
response to external stimulus
chemotaxis
regulation of cell proliferation in bone marrow
gland development
cell migration
positive regulation of transcription from RNA polymerase II promoter
Log10(1/P)
C
p65 target genes
R= -0.15
Il-6
Ccl5
Ccl2
Cxcl2
GTF2I
Ccl20
Log2 FC[(IL-6+IL-17 stimulation)/ (no stimulation)]
Log2 FC[GTF2I knockdown/MOCK]
D
STAT3 target genes
R= -0.025
Stat3
Log2FC[(IL-6+IL-17 stimulation)/ (no stimulation)]
Log2FC [GTF2I knockdown/MOCK]

Figure 6

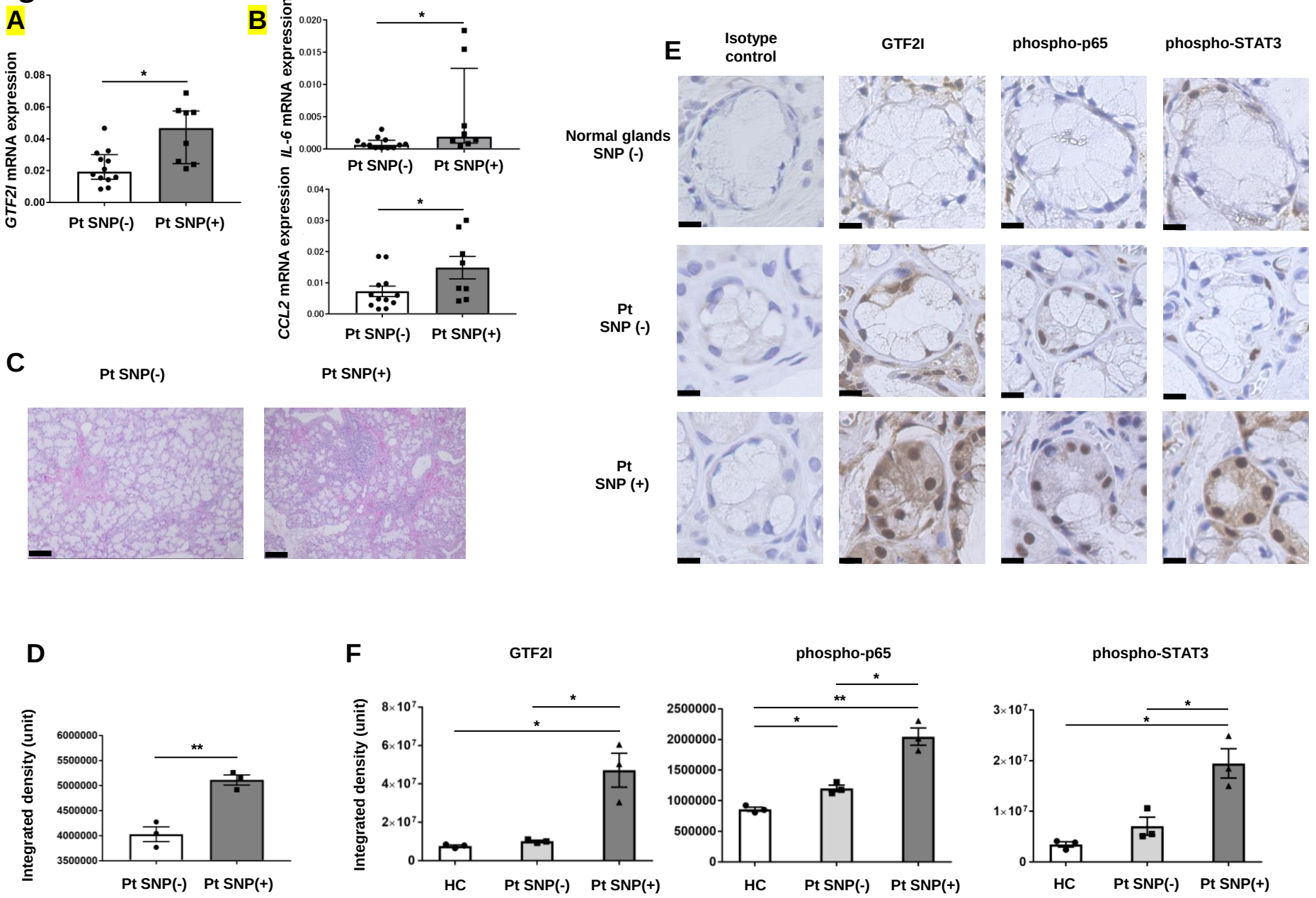
A
GTF2I mRNA expression
0.08
0.06
0.04
0.02
0.00
*
Pt SNP(-)
Pt SNP(+)
B
IL-6 mRNA expression
0.020
0.015
0.010
0.005
0.000
*
Pt SNP(-)
Pt SNP(+)
CCL2 mRNA expression
0.04
0.03
0.02
0.01
0.00
*
Pt SNP(-)
Pt SNP(+)
C
Pt SNP(-)
Pt SNP(+)
E
Isotype control
GTF2I
phospho-p65
phospho-STAT3
Normal glands SNP (-)
Pt SNP (-)
Pt SNP (+)
D
Integrated density (unit)
6000000
5500000
5000000
4500000
4000000
3500000
**
Pt SNP(-)
Pt SNP(+)
F
GTF2I
Integrated density (unit)
8×10^7
6×10^7
4×10^7
2×10^7
0
*
*
HC
Pt SNP(-)
Pt SNP(+)
phospho-p65
2500000
2000000
1500000
1000000
500000
0
*
**
*
HC
Pt SNP(-)
Pt SNP(+)
phospho-STAT3
3×10^7
2×10^7
1×10^7
0
*
*
HC
Pt SNP(-)
Pt SNP(+)